# Synthesis and gas adsorption properties of mesoporous silica-NH2-MIL-53(Al) core-shell spheres

Sorribas, S; Zornoza, B; Serra Crespo, P; Gascon, J; Kapteijn, F

**DOI**
10.1016/j.micromeso.2015.12.004

**Publication date**
2016

**Document Version**
Final published version

**Published in**
Microporous and Mesoporous Materials

Microporous and Mesoporous Materials 225 (2016) 116–121

Contents lists available at ScienceDirect

Microporous and Mesoporous Materials

journal homepage: www.elsevier.com/locate/micromeso

# Synthesis and gas adsorption properties of mesoporous silica-$NH_2$-MIL-53(Al) core–shell spheres

Sara Sorribas [a], Beatriz Zornoza [a], Pablo Serra-Crespo [b], Jorge Gascon [c], Freek Kapteijn [c], Carlos Téllez [a], Joaquín Coronas [a, *]

[a] Chemical and Environmental Engineering Department and Instituto de Nanociencia de Aragón (INA), Universidad de Zaragoza, 50018 Zaragoza, Spain
[b] Radiation and Isotopes for Health-Radiation Science and Technology, Delft University of Technology, Mekelweg 15, 2629 JB, Delft, The Netherlands
[c] Catalysis Engineering-Chemical Engineering Department, Delft University of Technology, Julianalaan 136, 2628 BL, Delft, The Netherlands

ARTICLE INFO

*Article history:*
Received 24 September 2015
Received in revised form
10 November 2015
Accepted 4 December 2015
Available online 17 December 2015

*Keywords:*
Metal-organic framework
$NH_2$-MIL-53
Ordered mesoporous silica
Core–shell
Adsorption

ABSTRACT

Ordered mesoporous silica-$NH_2$-MIL-53(Al) core–shell spheres of about 4 μm in diameter have been synthesized by seeding the corresponding mesoporous silica spheres (MSSs) with crystals of $NH_2$-MIL-53(Al) and subsequent secondary crystal growth into a MOF shell. The morphology of the particles was analyzed by SEM, while TGA, EDX and XRD characterizations gave information on the composition and structure of this material and the activation of the MOF. $N_2$ adsorption analysis revealed that the $NH_2$-MIL-53(Al) shell controlled the access of guest molecules into the hydrophilic silica mesoporous structure, while the breathing behavior of the microporous $NH_2$-MIL-53(Al) shell was confirmed by $CO_2$ adsorption isotherms.



## 1. Introduction

Metal–organic frameworks (MOFs) are emerging as a class of promising crystalline porous materials based on metal clusters or ions joined through organic linkers. Their structures, which can be designed according to targeted properties, as well as their high porosity and internal surface area, make these materials very attractive for several applications, including gas and mechanical energy storage [1,2], separation [3], sensing [4], catalysis [5] and drug delivery [6]. Two types can be found among the most important subfamilies of MOFs: ZIFs (zeolite imidazolate frameworks), where the metal ions or clusters are linked by imidazolate ligands [7], and metal carboxylate MOFs [8]. In the field of metal carboxylates, the use of the linear organic linker terephthalate can give rise to MOFs such as MIL-53 [9] and MIL-88B [10], which possess framework flexibility. By replacing terephthalic acid with 2-aminoterephthalic acid, the amino-functionalized forms of these and other MOFs (e.g. $NH_2$-MIL-53, $NH_2$-MIL-88B, $NH_2$-MIL-68) are obtained, showing different breathing behavior and gas adsorption properties [11–13].

Many efforts in material synthesis have been dedicated to tailor the size and shape of MOFs. Concerning the aforementioned $NH_2$-MIL-53, it has been prepared as nano-sized [11,14] and micro-sized [15–17] crystals as well as intergrown films [18], micro-needles and nanorods [19]. Furthermore, by altering the ratio of water in the DMF-water mixed synthesis solution, the size and morphology of $NH_2$-MIL-53 particles have been controlled [20]. The fabrication of MOFs in hollow sphere shape has been also published in the case of $Cu_3(BTC)_2$ [21], ZIF-8 [22], MIL101(Fe) [23] and Fe-soc-MOF [24].

Hierarchical structuring of MOF materials has emerged as an area of significant interest, the studies published being numerous and listed in several reviews [25–28]. For instance, previously in our group the fabrication of ordered mesoporous silica-ZIF-8 spheres combining ordered meso- and microporosity giving rise to core–shell structures was addressed [29]. Analogous composite materials have been used as stationary phase for HPLC, taking advantage of the good column packing properties of the uniform monodisperse silica microspheres and the separation ability of the MOF crystals [30,31], and as filler for the preparation of mixed matrix membranes applied in gas separation [32] and pervaporation [33,34]. A different approach has been reported for the MOF-silica core–shell materials, where different MOFs (i.e. ZIF-7, ZIF-8, UiO-66 and HKUST-1) were reinforced with shells of mesoporous

* Corresponding author. Tel.: +34 976762471; fax: +34 976761879.
*E-mail address:* coronas@unizar.es (J. Coronas).

http://dx.doi.org/10.1016/j.micromeso.2015.12.004
1387-1811/

silica, showing significant enhancement in mechanical properties (hardness and toughness) [35].

Following the idea of synthesizing hierarchical micro/mesoporous composites, the formation of mesoporous silica-$NH_2$-MIL-53(Al) core–shell particles has been studied here by application of seeding and subsequent secondary growth processes using MCM-41 mesoporous spheres as template and support. Interestingly, due to the breathing effect of $NH_2$-MIL-53(Al), the MOF shell can control the access of molecules such as $CO_2$ into the mesoporosity of the silica core.

## 2. Experimental

### 2.1. Synthesis of $NH_2$-MIL-53(Al) seeds

For the synthesis of $NH_2$-MIL-53(Al) seeds, the molar gel composition of $Al^{3+}$: ($NH_2$–$H_2BDC$): DMF = 1: 1.37: 99 was used [36]. For that, 0.78 g of aluminum nitrate nonahydrate ($Al(NO_3)_3 \cdot 9H_2O$, >98%, Aldrich) and 0.564 g of 2-aminoterephthalic acid ($NH_2$–$H_2BDC$, 99%, Aldrich) were dissolved in 30 mL of N,N-dimethylformamide (DMF, >95%, Scharlau). The solution was transferred to a Teflon-lined autoclave (45 mL capacity) and treated at 130 °C for 3 days in a Memmert oven. The product was washed with acetone and activated with methanol at 75 °C overnight. The solid was collected by centrifugation and dried at 100 °C.

### 2.2. Synthesis of seeded mesoporous silica spheres with $NH_2$-MIL-53(Al) crystals

Mesoporous silica spheres (MSSs) with MCM-41 structure were prepared following the literature [29,37]. Briefly, the molar composition used was $Na_2SiO_3$: CTABr: $H_2O$: $CH_3COOC_2H_5$ = 1.5: 1: 361: 7.4. For that, 3.92 g of cetyltrimethylammonium bromide (CTABr, >98%, Sigma–Aldrich) and 2 g of sodium metasilicate ($Na_2SiO_3$, Sigma–Aldrich) were dissolved in 70 mL of distilled water. After that, 8 mL of ethylacetate ($CH_3COOC_2H_5$, 99.9% Sigma–Aldrich) was added under stirring for 30 s. The solution was kept in a closed polypropylene flask at room temperature for 5 h, and then treated at 90 °C for 50 h. The product obtained was filtered in distilled water and ethanol, and finally the sample was calcined at 600 °C for 8 h with a heating rate of 0.5 °C/min in order to remove the surfactant. The obtained MSSs presented a bimodal system of mesopores of 2.7 nm, characteristic of MCM-41 structure, and larger pores of about 15 nm, and the BET area was 940 ± 40 $m^2$/g.

For the seeding of MSSs with $NH_2$-MIL-53(Al) crystals, two different processes were developed. On the one hand, the *ex situ* seeding process in which $NH_2$-MIL-53(Al) seeds (0.1 g) were dispersed in 10 mL DMF and MSSs (0.2 g) were added. The mixture was sonicated for 15 min and stirred for 30 min and the solid was collected by centrifugation with DMF and acetone. For the *in situ* seeding process, 0.26 g $Al(NO_3)_3 \cdot 9H_2O$ and 0.188 g $NH_2$–$H_2BDC$ were dissolved in 10 mL of DMF. After that, 0.2 g MSSs was added and the dispersion was transferred to a 45 mL Teflon-lined autoclave. The synthesis was carried out in the oven at 130 °C for 3 days under rotating conditions (30 r.p.m). The product was washed with acetone, activated with methanol overnight and dried at 100 °C.

### 2.3. Synthesis of mesoporous silica-($NH_2$-MIL-53(Al)) spheres

For the regrowth of seeded MSSs, a molar gel composition of $1Al^{3+}$: $1NH_2$–$H_2BDC$: $153H_2O$ was used as follows [38]: 0.25 g of aluminum chloride hexahydrate ($AlCl_3 \cdot 6H_2O$, 99%, Sigma–Aldrich) was mixed with 0.187 g of $NH_2$–$H_2BDC$ and 10 mL of $H_2O$. Then, 0.1 g of MSSs was added and the synthesis was carried out in an autoclave at 150 °C for 5 h under rotation. The sample containing free aminoterephthalic acid was activated following two steps. In the first, the unreacted aminoterephthalic acid was exchanged by DMF at 150 °C, while in the second the DMF molecules were removed by washing several times with acetone and then with methanol. Finally, the product was dried at 100 °C overnight for characterization.

### 2.4. Characterization

MOF particle size and silica-$NH_2$-MIL-53(Al) spheres morphology were characterized by scanning electron microscopy (SEM) using an Inspect F scanning electron microscope. Prior to observation, the samples were sputter coated with 15 nm platinum. To distinguish the Al of the MOF and the Si of the silica spheres, EDX mapping was also carried out. Transmission electron microscopy (TEM) images were recorded on a FEI TECNAI T20 at an acceleration voltage of 200 kV. To prepare samples for TEM, the solid was suspended in ethanol and placed in an ultrasound bath for 10 min. A drop of this suspension was poured on a copper grid (200 mesh) coated with carbon film and allowed to dry in air.

Thermogravimetric analyses (TGA) were performed on Mettler Toledo TGA/DTA 1 Start system equipment. Samples (10 mg) placed in 70 μL alumina pans were heated in an air flow (96 $cm^3$(STP)/min) up to 800 °C at a heating rate of 10 °C/min to determine the mass percentage of MOF in the composite material after seeding and secondary growth processes.

High-pressure adsorption isotherms of pure $CO_2$ (purity of 99.995%) were determined at 0 °C by the volumetric technique (Belsorp HP) using 0.5 g of sample. Before every measurement, the previously activated solid was outgassed by increasing the temperature to 200 °C at a rate of 10 °C/min under vacuum and maintaining the temperature for 2 h.

Nitrogen adsorption–desorption isotherms were measured at −196 °C using a porosity analyzer (TriStar 3000, Micromeritics Instrument Corp., $N_2$ purity of 99.999%). The samples were outgassed under vacuum using a heating rate of 10 °C/min until 200 °C and maintained for 8 h.

The materials were also characterized by X-ray diffraction (XRD) at room temperature on a D-Max Rigaku diffractometer with a copper anode and a graphite monochromator to select Cu-$K_{\alpha 1}$ radiation (λ = 1.5418 Å). Zeta-potential measurements were performed on a Brookhaven Instruments 90 Plus equipment, employing the Smoluchowski equation. The samples were dispersed in distillate water using an ultrasound bath for 15 min and all the measurements were conducted at 25 °C.

## 3. Results and discussion

### 3.1. Seeding process

The XRD pattern of the synthesized $NH_2$-MIL-53(Al) seeds (Fig. 1) matches the $NH_2$-MIL-53_*np* form (narrow pore) [38], characteristic of activated samples. The particle size of $NH_2$-MIL-53(Al) seeds was 70 ± 17 nm (Fig. 2). Even though these images suggest agglomeration, this was due to the drying. Zeta potential values were measured in distillate water: −10 mV and 3.8 mV for MSSs and $NH_2$-MIL-53(Al), respectively. These values suggest electrostatic attraction between both materials in also polar DMF solvent (in which the seeding was carried out).

As explained in the experimental section, *ex situ* seeding refers to the process carried out by suspending $NH_2$-MIL-53(Al) seeds and MSSs in DMF at room temperature, while *in situ* seeding means that MSSs were added to the synthesis gel of $NH_2$-MIL-53(Al) seeds. The attraction between silica and $NH_2$-MIL-53(Al) observed by SEM in

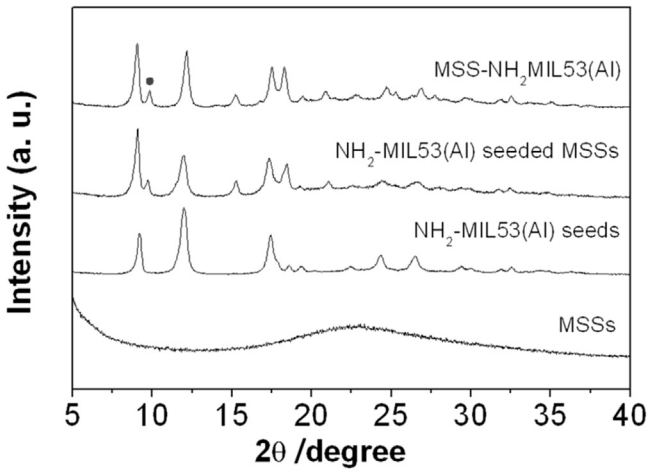


**Fig. 1.** XRD patterns of MSSs, $NH_2$-MIL-53(Al) seeds, $NH_2$-MIL-53(Al) seeded MSSs and MSS-$NH_2$MIL53(Al). The dot marks the peak corresponding to the "lp" structure.

both *ex situ* and *in situ* seeding procedures (Fig. 3) could be due to the hydrogen bonding interactions between the surface hydroxyls and amino groups of the MOF and the hydroxyl groups of silica. When the *in situ* seeding was carried out a higher coverage degree, MOF particles with an average size of 70 ± 14 nm were obtained, representing 62 wt% of the sample calculated by TGA (Figure S1). This particle size is similar to that corresponding to the $NH_2$-MIL-53(Al) seeds (Fig. 2). Due to the higher degree of coverage obtained and easiness, from now on the results will focus on *in situ* seeding.

### 3.2. Crystal growth

To create the $NH_2$-MIL-53(Al) shell around the MSSs and obtain mesoporous silica-($NH_2$-MIL-53(Al)) core–shell spheres (labelled MSS-$NH_2$MIL53(Al)), the synthesis procedure published by Ahnfeldt et al. [38] using water as solvent was used in the presence of *in situ* seeded MSSs. The use of water instead of DMF as solvent [20] led to $NH_2$-MIL-53(Al) with elongated shape and larger particle size (average length of 880 ± 30 nm, Fig. 4a). This can be explained by the fact that water inhibits the deprotonation of $NH_2$–$H_2$BDC, reducing its solubility and slowing down the nucleation rate. In consequence, this leads to increased crystal size and crystal anisotropy [20].

A homogeneous crystal shell is obtained after the $NH_2$-MIL-53(Al) growth procedure (Fig. 4b) with an average MOF particle size of 150 ± 25 nm. EDX line map, which intensity increased from right to left, represents aluminum concentration in red and silicon concentration in blue (Fig. 4c). A uniform distribution of the MOF coating over the surface of the spheres is observed, with different concentration profiles due to the silica thickness variation along the sphere, since EDX has a large interaction volume on the order of micrometers. TEM images (Figure S2) confirm the presence of both silica core and MOF crystals shell, in addition with some non-attached crystals outside the spheres which could not be removed by decantation in methanol.

As previously reported for mesoporous silica-(ZIF-8) spheres [29], when no seeding was applied no interaction between the micrometer $NH_2$-MIL-53(Al) crystals and the silica spheres was achieved, but instead a blend of MSSs and $NH_2$-MIL-53(Al) crystals was obtained (Figure S3).

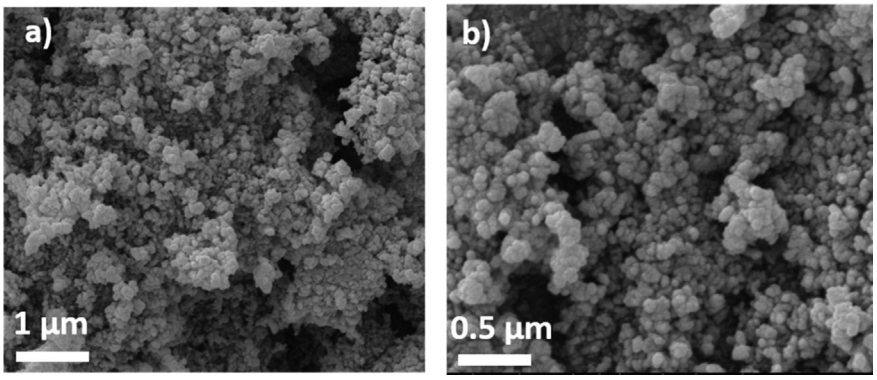


**Fig. 2.** SEM images of $NH_2$-MIL-53(Al) seeds.

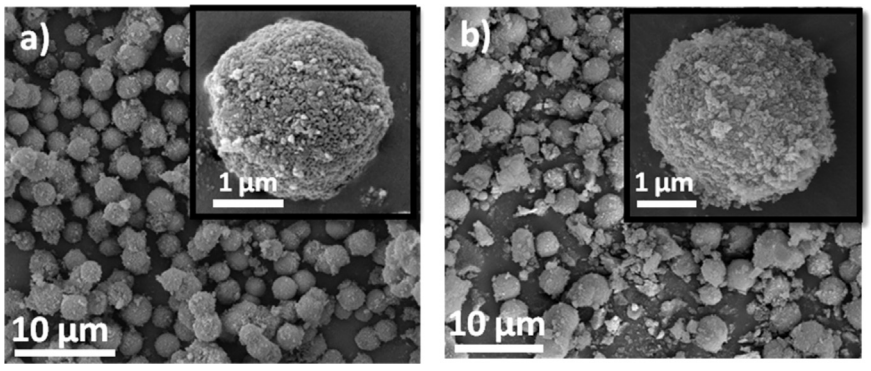


**Fig. 3.** SEM images of MSSs coated with $NH_2$-MIL-53(Al) crystals by a) *ex situ* seeding, b) *in situ* seeding.

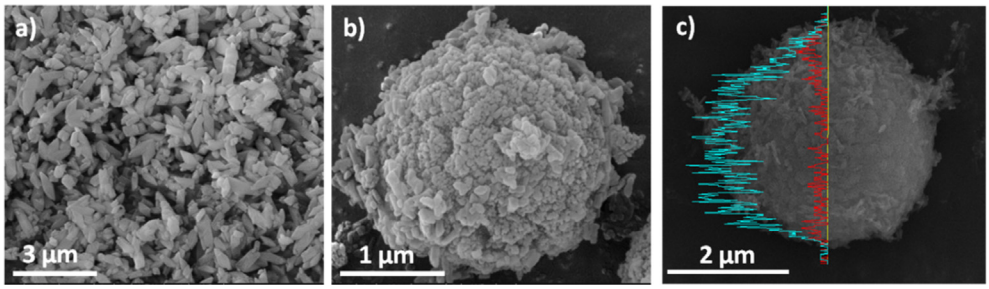


**Fig. 4.** SEM images of: a) $NH_2$-MIL-53(Al) crystals synthesized at 150 °C, 5 h in water; b) MSS-$NH_2$MIL53(Al) sphere after crystal growth; c) EDX line map of MSS-$NH_2$MIL53(Al) after crystal growth (red and blue are Al and Si, respectively). (For interpretation of the references to colour in this figure legend, the reader is referred to the web version of this article.)

The matching of the X-ray diffraction patterns obtained for the core–shell particles (both after seeding and crystal growth steps) with that corresponding to the $NH_2$-MIL-53_*np* form demonstrates the formation of the $NH_2$-MIL-53 phase (see Fig. 1). Note that the characteristic peaks for both the *lp* structure at $2\theta = 9.5°$ (marked with a red dot) and the *np* structure at $2\theta = 12°$ can be observed in both samples, $NH_2$-MIL-53(Al) seeded MSSs and MSS-$NH_2$MIL53(Al). This indicates the coexistence of both forms [11], probably due to the presence of free aminoterephthalic acid or DMF molecules in the pores that were not completely removed during the activation step (i.e. with DMF at 150 °C overnight and then under reflux with MeOH for 10 h and dried at 100 °C). Besides, the lowest angle peak ($2\theta < 9.5°$), corresponding also to the *np* structure, remains unchanged for all the samples.

A further low-angle XRD analysis to the MSS-$NH_2$MIL53(Al) (Figure S4) suggested that the ordered MCM-41 structure present in the silica template disappeared during the seeding and growing processes leading to a disordered material. The same effect occurs when functionalizing silica microspheres by means of a Grignard surface modification treatment [39]. We do not have direct evidence of the damage (densification) of the mesoporous structure during the seeding stage, as happen in case of other analogous seeding processes for core shell particles [29,40].

Thermogravimetry analyses in air (Figure S1) confirm that the $NH_2$-MIL-53(Al) seeds and MSS-$NH_2$MIL53(Al) samples were stable up to approximately 400 °C, in agreement with the TGA reported for the solvent-free $NH_2$-MIL-53 structure [38]. These analyses also allowed the calculation of the percentage of MSSs and MOF present in the MSS-$NH_2$MIL53(Al) sample after the secondary growth, corresponding to 19 wt% and 81 wt%, respectively.

### 3.3. $N_2$ and $CO_2$ adsorption properties of MSS-$NH_2$MIL53(Al)

Fig. 5 shows the $N_2$ sorption isotherms of $NH_2$-MIL-53(Al) seeds, MSSs and MSS-$NH_2$MIL53(Al) samples. $N_2$ interacted weakly with the $NH_2$-MIL-53(Al) seeds, and since the MOF was present in the $NH_2$-MIL-53_*np* form, $N_2$ could not adsorb at low pressure [41]. The $N_2$ adsorbed in this sample at high relative pressures was related to the capillary condensation between adjacent nanocrystals. This was more significant for the MSS-$NH_2$MIL53(Al) sample, in which the intercrystalline spaces between the $NH_2$-MIL-53(Al) crystals forming the shell contributed to the capillary condensation. As previously observed, $N_2$ adsorption on $NH_2$-MIL-53 material strongly depends on the particle size and pretreatment conditions. As an example, Cheng et al. observed different $N_2$ adsorption isotherms and BET areas by tuning the water ration in the DMF-water mixed solvent during the $NH_2$-MIL-53 synthesis [20].

The increase in the adsorbed volume at $p/p_o = 0.30–0.35$ present in the MSSs as well as the hysteresis loop related to larger mesopores were not present in the MSS-$NH_2$MIL53(Al) isotherm, since the $NH_2$-MIL-53(Al) shell precluded entering of $N_2$ into the remaining porosity of the silica core, suggesting a continuous intergrowth coating of the MOF.

To compare the $CO_2$ adsorption properties of microporous $NH_2$-MIL-53(Al) crystals, MSSs and MSS-$NH_2$MIL53(Al) comprising both mesoporous core and microporous shell and to study the breathing phenomenon of $NH_2$-MIL-53(Al) and MSS-$NH_2$MIL53(Al) samples, the $CO_2$ adsorption up to 3.5 MPa (35 bar) at 0 °C was studied (Fig. 6).

At pressures below 0.5 MPa, the $CO_2$ adsorption in $NH_2$-MIL-53(Al) sample reached ~2.5 mmol/g, which represents ~0.5 $CO_2$ per µOH [15]. The drastic increase in the amount of $CO_2$ adsorbed occurred at pressures higher than 1.2 MPa, where the opening of the material (*np*-*lp* transition) takes place. The higher pressure needed to reopen the pore structure in comparison with MIL-53(Al), which was reported to be 0.5 MPa [42,43], is related to the stronger interaction within the framework ($NH_2 \leftrightarrow$OH interaction) which leads to a partial contraction of the framework, and thus to a smaller effective pore size [11,12].

Regarding MSSs, the $CO_2$ adsorption reached ~1 mmol/g at pressures about 0.1 MPa and at higher pressures the $CO_2$ uptake increased almost linearly with increasing $CO_2$ pressure, in accordance with literature for MCM-41 silica [44]. At pressures above 3.0 MPa the $CO_2$ uptake increased drastically, reaching 16 mmol/g.

For MSS-$NH_2$MIL53(Al), the $CO_2$ adsorption reached ~2 mmol/g at about 0.1 MPa. The measured gate opening pressure (~1.75 MPa) was higher than the value of 1.2 MPa for $NH_2$-MIL-53(Al). While for the $NH_2$-MIL-53(Al) sample the amount of $CO_2$ adsorbed drastically

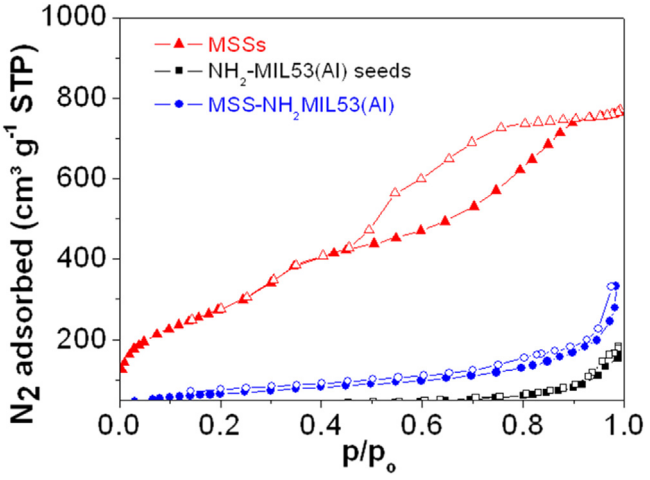


**Fig. 5.** Adsorption–desorption isotherms of $N_2$ at −196 °C for MSSs, $NH_2$-MIL-53(Al) seeds and MSS-$NH_2$MIL53(Al) samples. Solid and open symbols correspond to adsorption and desorption, respectively.

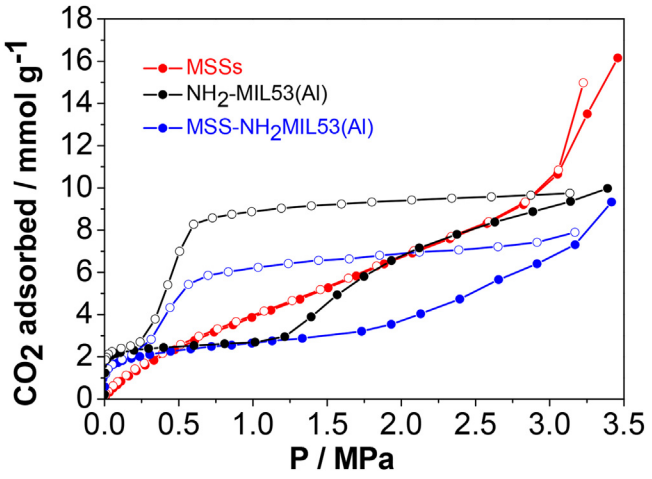


**Fig. 6.** Adsorption–desorption isotherms of $CO_2$ at 0 °C for MSSs, $NH_2$-MIL-53(Al) and MSS-$NH_2$MIL53(Al) samples. Solid and open symbols correspond to adsorption and desorption, respectively.

increased at 1.2 MPa because of the *np* to *lp* transition, for MSS-$NH_2$MIL53(Al) this increase was more progressive. This fact suggests that $NH_2$-MIL-53(Al) crystals may act as a barrier for $CO_2$ to enter into the mesopores of the silica core. Once the MOF pores were fully open at high pressure, $CO_2$ molecules accessed to the pores of the silica increasing the $CO_2$ adsorption. It should also be taken into account that different crystallite sizes and crystals distribution leads to different isotherm profiles, as reported by Lescouet et al. [15]. Since $NH_2$-MIL-53(Al) consists of isolated crystals of 70 nm in size and in MSS-$NH_2$MIL53(Al) sample the obtained crystals are 150 nm in size and are aggregated at the external surface of the spheres (Fig. 4b), the particle size and aggregation morphology could also explain the different $CO_2$ adsorption profiles. At the highest $CO_2$ partial pressure tested (about 3.5 MPa) $NH_2$-MIL53(Al) and MSS-$NH_2$MIL53(Al) had similar adsorption values of *ca* 10 mmol/g, in agreement with the contribution of the silica mesoporosity to the total $CO_2$ capacity of the core–shell particle. This total adsorption value is a little lower than that estimated by individual contributions based on the composition of the core–shell system (19 wt% MSSs and 81 wt% MOF, see Figure S5), probably due to some loss in the porosity of MSSs during the MOF synthesis process, as observed by low-angle XRD (Figure S2). The difference in shape of the isotherm curves MSS-$NH_2$MIL53(Al) and simulation (considering physical mixture) demonstrates again the core–shell structure of this composite material. Finally, the particles appeared broken at the end of the $CO_2$ adsorption experiments, probably due to the mechanical stress suffered after the MOF breathing; this did not allow cycling experiments.

## 4. Conclusions

The synthesis of mesoporous silica-($NH_2$-MIL-53(Al)) core–shell spheres using seeding and secondary crystal growth has been reported. The *in situ* seeding process provided a higher coverage degree, with 62 wt% of MOF, and this percentage increased up to 81 wt% after the secondary growth. The formation of a continuous $NH_2$-MIL-53(Al) shell, in which the breathing behavior of the MOF controls the entrance of guest molecules into the silica core, was assessed by $N_2$ and $CO_2$ adsorption measurements. This controlled uptake makes this new composite material very interesting for applications such as encapsulation or gas separation processes. Finally, at the highest $CO_2$ partial pressure tested (about 3.5 MPa) the silica-MOF and MOF samples have a similar adsorption of *ca* 10 mmol/g.

## Acknowledgments

Financial support from the Spanish Ministry of Economy and Competitiveness (MAT2013-40556-R), DGA Program fellowships (S. S.) from the Regional Government of Aragón and the ESF are gratefully acknowledged. We acknowledge the use Servicio General de Apoyo a la Investigación-SAI (Universidad de Zaragoza). All the microscopy work was done in the Laboratorio de Microscopías Avanzadas at the Instituto de Nanociencia de Aragón (LMA-INA). The authors acknowledge the LMA-INA for offering access to their instruments and expertise.

## Appendix A. Supplementary data

Supplementary data related to this article can be found at http://dx.doi.org/10.1016/j.micromeso.2015.12.004.

## References

[1] M. Latroche, S. Surblé, C. Serre, C. Mellot-Draznieks, P.L. Llewellyn, J.-H. Lee, J.-S. Chang, S.H. Jhung, G. Férey, Angew. Chem. Int. Ed. 45 (2006) 8227–8231.
[2] G. Ortiz, H. Nouali, C. Marichal, G. Chaplais, J. Patarin, J. Phys. Chem. C 118 (2014) 7321–7328.
[3] B. Zornoza, C. Tellez, J. Coronas, J. Gascon, F. Kapteijn, Microporous Mesoporous Mater. 166 (2013) 67–78.
[4] M.D. Allendorf, R.J.T. Houk, L. Andruszkiewicz, A.A. Talin, J. Pikarsky, A. Choudhury, K.A. Gall, P.J. Hesketh, J. Am. Chem. Soc. 130 (2008) 14404–14405.
[5] D.Y. Hong, Y.K. Hwang, C. Serre, G. Férey, J.S. Chang, Adv. Funct. Mater. 19 (2009) 1537–1552.
[6] N. Liedana, P. Lozano, A. Galve, C. Tellez, J. Coronas, J. Mater. Chem. B 2 (2014) 1144–1151.
[7] K.S. Park, Z. Ni, A.P. Cote, J.Y. Choi, R.D. Huang, F.J. Uribe-Romo, H.K. Chae, M. O'Keeffe, O.M. Yaghi, Nat. Acad. Sci. U. S. A. 103 (2006) 10186–10191.
[8] C. Livage, C. Egger, M. Nogues, G. Ferey, J. Mater. Chem. 8 (1998) 2743–2747.
[9] T. Loiseau, C. Serre, C. Huguenard, G. Fink, F. Taulelle, M. Henry, T. Bataille, G. Ferey, Chem. Eur. J. 10 (2004) 1373–1382.
[10] S. Surble, C. Serre, C. Mellot-Draznieks, F. Millange, G. Ferey, Chem. Commun. (2006) 284–286.
[11] A. Boutin, S. Couck, F.-X. Coudert, P. Serra-Crespo, J. Gascon, F. Kapteijn, A.H. Fuchs, J.F.M. Denayer, Microporous Mesoporous Mater. 140 (2011) 108–113.
[12] E. Stavitski, E.A. Pidko, S. Couck, T. Remy, E.J.M. Hensen, B.M. Weckhuysen, J. Denayer, J. Gascon, F. Kapteijn, Langmuir 27 (2011) 3970–3976.
[13] L. Wu, M. Xue, S.-L. Qiu, G. Chaplais, A. Simon-Masseron, J. Patarin, Microporous Mesoporous Mater. 157 (2012) 75–81.
[14] S. Couck, J.F.M. Denayer, G.V. Baron, T. Remy, J. Gascon, F. Kapteijn, J. Am. Chem. Soc. 131 (2009) 6326.
[15] T. Lescouet, E. Kockrick, G. Bergeret, M. Pera-Titus, D. Farrusseng, Dalton Trans. 40 (2011) 11359–11361.
[16] J. Kim, W.Y. Kim, W.S. Ahn, Fuel 102 (2012) 574–579.
[17] B. Zornoza, A. Martinez-Joaristi, P. Serra-Crespo, C. Tellez, J. Coronas, J. Gascon, F. Kapteijn, Chem. Commun. 47 (2011) 9522–9524.
[18] H. Fan, H. Xia, C. Kong, L. Chen, Int. J. Hydrogen Energy 38 (2013) 10795–10801.
[19] J.M. Chin, E.Y. Chen, A.G. Menon, H.Y. Tan, A.T.S. Hor, M.K. Schreyer, J. Xu, Cryst. Eng. Commun. 15 (2013) 654–657.
[20] X. Cheng, A. Zhang, K. Hou, M. Liu, Y. Wang, C. Song, G. Zhang, X. Guo, Dalton Trans. 42 (2013) 13698–13705.
[21] R. Ameloot, F. Vermoortele, W. Vanhove, M.B.J. Roeffaers, B.F. Sels, D.E. De Vos, Nat. Chem. 3 (2011) 382–387.
[22] H.J. Lee, W. Cho, M. Oh, Chem. Commun. 48 (2012) 221–223.
[23] A.L. Li, F. Ke, L.G. Qiu, X. Jiang, Y.-M. Wang, X.-Y. Tian, Cryst. Eng. Commun. 15 (2013) 3554–3559.
[24] M. Pang, A.J. Cairns, Y. Liu, Y. Belmabkhout, H.C. Zeng, M. Eddaoudi, J. Am. Chem. Soc. 135 (2013) 10234–10237.
[25] Q.L. Zhu, Q. Xu, Chem. Soc. Rev. 43 (2014) 5468–5512.
[26] C.M. Doherty, D. Buso, A.J. Hill, S. Furukawa, S. Kitagawa, P. Falcaro, Acc. Chem. Res. 47 (2013) 396–405.
[27] S. Furukawa, J. Reboul, S. Diring, K. Sumida, S. Kitagawa, Chem. Soc. Rev. 43 (2014) 5700–5734.
[28] B. Seoane, S. Castellanos, A. Dikhtiarenko, F. Kapteijn, J. Gascon, Coord. Chem. Rev. 307 (2016) 148–187.
[29] S. Sorribas, B. Zornoza, C. Tellez, J. Coronas, Chem. Commun. 48 (2012) 9388–9390.
[30] Y.Y. Fu, C.X. Yang, X.-P. Yan, Chem. Eur. J. 19 (2013) 13484–13491.
[31] A. Ahmed, M. Forster, R. Clowes, D. Bradshaw, P. Myers, H. Zhang, J. Mater. Chem. A 1 (2013) 3276–3286.
[32] S. Sorribas, B. Zornoza, C. Tellez, J. Coronas, J. Membr. Sci. 452 (2014) 184–192.
[33] Y.C. Sue, J.W. Wu, S.E. Chung, C.H. Kang, K.L. Tung, K.C.W. Wu, F.K. Shieh, Acs Appl. Mat. Inter. 6 (2014) 5192–5198.

[34] A. Kudasheva, S. Sorribas, B. Zornoza, C. Téllez, J. Coronas, J. Chem. Technol. Biot. 90 (2014) 669–677.
[35] Z. Li, H.C. Zeng, J. Am. Chem. Soc. 136 (2014) 5631–5639.
[36] S. Sorribas, P. Gorgojo, C. Tellez, J. Coronas, A.G. Livingston, J. Am. Chem. Soc. 135 (2013) 15201–15208.
[37] G. Schulz-Ekloff, J. Rathousky, A. Zukal, Int. J. Inorg. Mater. 1 (1999) 97–102.
[38] T. Ahnfeldt, D. Gunzelmann, T. Loiseau, D. Hirsemann, J. Senker, G. Ferey, N. Stock, Inorg. Chem. 48 (2009) 3057–3064.
[39] B. Zornoza, C. Téllez, J. Coronas, O. Esekhile, W.J. Koros, AIChE J. 61 (2015) 4481–4490.
[40] N. Navascues, C. Téllez, J. Coronas, Microporous Mesoporous Mater. 112 (2008) 561–572.
[41] S. Couck, E. Gobechiya, C.E.A. Kirschhock, P. Serra-Crespo, J. Juan-Alcañiz, A. Martinez Joaristi, E. Stavitski, J. Gascon, F. Kapteijn, G.V. Baron, J.F.M. Denayer, Chem. Sus. Chem. 5 (2012) 740–750.
[42] S. Bourrelly, P.L. Llewellyn, C. Serre, F. Millange, T. Loiseau, G. Férey, J. Am. Chem. Soc. 127 (2005) 13519–13521.
[43] P.L. Llewellyn, S. Bourrelly, C. Serre, Y. Filinchuk, G. Férey, Angew. Chem. Int. Ed. 45 (2006) 7751–7754.
[44] Y. Belmabkhout, A. Sayari, Adsorption 15 (2009) 318–328.